Published in final edited form as:
Opt Lett. 2010 August 15; 35(16): 2735–2737.

Endoscope lens with dual fields of view and resolutions for multiphoton imaging

Minghan Chen[1,*], **Chris Xu**[1,2], and **Watt W. Webb**[1]

[1] School of Applied and Engineering Physics, Cornell University, Ithaca, New York 14853, USA

Abstract

We report the development of a miniaturized dual-optical-zone endoscope objective lens. The lens has two foci, with 0.18 and 0.50 NAs. We demonstrate multiphoton imaging with dual fields of view and resolutions using the new lens. A combination of multiphoton and single-photon microscopic imaging is also demonstrated.

Multiphoton microscopy (MPM) is a powerful tool for biological imaging [1]. It enables minimally invasive imaging of endogenous fluorescent species and harmonic generation [2], providing contrast in unstained tissues. By incorporating a miniaturized endoscope, medical multiphoton microscopic endoscopy (MPM-E) could play a significant role in clinical cancer diagnosis. As presented in previous reports of multiphoton microscopic endoscopes [3,4], MPM-E can facilitate noninvasive diagnosis of a diseased state *in situ*, potentially becoming a valuable technology for clinical diagnosis.

A significant obstacle to the development of a practical MPM-E probe has been the need for optical zooming capability. During clinical diagnosis, low-magnification and large field of view (FOV) imaging would allow clinicians to survey a large area and locate the disease site and then perform high-resolution multiphoton imaging to confirm the diagnosis. For practical implementation, both the large FOV imaging and high-resolution imaging must be obtained with the same endoscope apparatus. While such an optical zooming capability is easily accomplished with conventional microscopes by using multiple objective lenses, achieving the same capability in a compact endoscope presents a significant challenge. Previous fiber based MPM-E designs [3–6] utilized either monolithic components, such as gradient refractive index (GRIN) lenses, or compound lens assembly [7]. However, these endoscope probes do not provide optical zooming capability. Although by scanning a small area using a galvo mirror or fiber scanner, magnified images could be obtained. However, this magnification does not change optical resolution. Therefore, previous systems were limited to performing *either* high-resolution imaging with a small FOV *or* low-resolution imaging with a large FOV. We present in this Letter a method of employing a bifocal endoscope objective lens for multi-photon microscopic imaging. The lens has two foci and enables imaging with two different magnifications, resolutions, and FOVs without the need for any mechanical or optical adjustment of the internal endoscope components.

The lens assembly was designed with Zemax software, and the ray-tracing diagram is illustrated in Fig. 1(a). Light emitting from a point source is focused by the lens assembly into two foci simultaneously with two different NAs. The lens assembly includes a collimating lens and a bifocal lens. The collimating lens was fabricated from a commercial

[*]Corresponding author: mc857@cornell.edu.
[2]cx10@cornell.edu

lens (Edmund Optics NT46-342) by cutting down the peripheral areas of the lens so that a diameter of 4 mm is achieved. The bifocal lens was fabricated by first cutting an asphere lens (Edmund Optics NT-46343) into 4 mm diameter. Then, a center through-hole (5 mm length) was drilled, and a GRIN objective (GRINTECH GmbH) of 5 mm length was cemented into the through hole. The collimation lens and the focusing lens are in physical contact with each other. Figure 1(b) shows the fabricated bifocal objective lens assembly. The lens outer diameter is 4.0 mm. The central optical zone is around 2 mm diameter, while the peripheral optical zone covers the remaining lens area. For a focal point with the 0.5 NA central zone, the Strehl ratios are 0.98, 0.50, and 0.25 at the center, 0.7, and full FOV (188 μm), respectively, which are typical of a GRIN objective. For a focal point with the 0.18 NA peripheral zone, the Strehl ratios are 0.89, 0.71 and 0.3 at the center, 0.7, and full FOV, respectively. At the peripheral area of the FOV, astigmatism and coma are the major aberrations. We note that the bifocal lens assembly was fabricated using low-cost, commercially available lenses to demonstrate the feasibility of optical zooming. Off-axis aberrations can be significantly reduced by using customized lenses.

Using 800 nm center wavelengths and assuming a 10 nm bandwidth, the calculated focal plane axial chromatic shifts are 1.4 and 8 μm for the 0.5 and 0.18 NA foci, respectively. Maximal lateral colors (lateral chromatic shift of the focus) at the image plane (at the largest FOV) are 0.006 and 0.02 μm for the 0.18 and 0.5 NA foci, respectively. These values are much smaller than the sizes of both foci. Furthermore, the values are significantly smaller than the pulse length in space (e.g., 30 μm for a 100 fs pulse). Thus, chromatic aberration will not cause significant spatial and temporal distortion at the focus.

Figure 2 shows the instrument setup for acquiring reflection/multiphoton images with large FOV/low resolution and small FOV/high resolution. Switching between the two imaging modes does not require any optical or mechanical alteration of the imaging system, enabling a compact and convenient configuration for MPM-E. By adjusting the relative distance between the endoscope assembly and the sample along the optical axis without lateral motion, the high-resolution image obtained was exactly at the center of the larger FOV image. In practice, lateral motion may need to be incorporated in the translation process to account for the possible motion of the object.

To characterize the lateral resolution, we examined the endoscope objective lens with a U.S. Air Force (USAF) target using one-photon reflection imaging. Figure 3(a) shows the measured reflection image of a USAF target. To characterize the resolution limit of the lens, magnified images were obtained by scanning a small area in the center of the FOV. With a 0.18 NA, the simulated resolution is ~2.14 μm, which is close to the width of the group 7 element 6 (2.19 μm) [highlighted using the dashed rectangle in Fig. 3(a)]. Reflection images with the higher resolution (0.50 NA) were also measured with bars in groups 8 and 9 [Fig. 3(b)]. As indicated with the dashed rectangle in Fig. 3(b), the bar width of 0.977 μm can be resolved, which agrees very well with the theoretical resolution of 0.976 μm for a 0.5 NA optical system using 800 nm laser light.

Because the two foci of the bifocal lens are located coaxially along the optical axis, cross talk between the foci is a concern. The inherent axial sectioning capability of MPM [1] ensures that there is negligible out-of-focus background generation, removing the cross talk between the two imaging modes. Thus, multiphoton imaging is naturally well suited for such a bifocal lens design. We characterized the lens axial resolution of the optical system by scanning through the center of 0.2 μm beads along the axial direction using a translation stage. As shown in Fig. 4, two foci were observed along the optical axis, with a separation of 7.8 mm. The fluorescence intensity of each focus was normalized and fitted with a Gaussian profile shown by the insets. The FWHM of the axial response for the 0.5 and 0.18 NA

optical zones are 5.8 and 56 μm, respectively. The FWHM value of the 0.5 NA focus is close to the theoretical prediction of 4.63 μm. The small difference between the experiment and the theory is likely due to the chromatic aberration of the lens assembly. Figure 4 clearly shows that the cross talk is negligible, and the presence of the second focus has negligible impact on multiphoton imaging. Similar to multiphoton imaging, a confocal pinhole can be added to reduce the cross talk of the two foci in single-photon imaging.

Figures 5(a) and 5(b) shows multiphoton images of 6 μm fluorescence beads fixed in agarose using the bifocal lens. In the low-resolution and large FOV image, a large amount of beads was observed with an FOV of approximately 1 mm × 1 mm, while the high-resolution image could identify the detailed features of individual beads clearly with a smaller FOV of 188 μm × 188 μm. An average of 2 mW of laser power was focused at the sample, and both images were taken at a frame rate of 1 Hz. In addition to fluorescent beads, the second-harmonic generation (SHG) images of the collagen fibers of a rat-tail tendon were also obtained and are shown in Figs. 6(a) and 6(b). The diameter of the entire collagen fiber is approximately 153 μm, as indicated in Fig. 6(a) using the low-NA peripheral imaging zone. After zooming in using the center high-NA optical zone, fine tendon structures are clearly resolved. The individual collagen fiber bundles are closely packed, with a diameter of approximately 1.3 μm for each bundle, which agrees very well with the value reported in the previous literature [8]. About 4 and 13 mW of laser power were focused onto the rat-tail samples with the 0.5 and 0.18 NA, respectively. Because the laser beam is divided into two separate foci, compared with a conventional lens, a relatively higher laser power (approximately 1.5 times) needs to be used with the bifocal lens. We also performed one-photon reflection imaging of the rat-tail fibers, and the results are shown in Figs. 6(c) and 6(d). Specular reflection, which is the reflection of light from the glass substrate, was observed in both images, which could be largely eliminated by using a confocal pinhole. SHG images show better contrast than that of reflection images with both NAs. Our experiments showed that a combination of one-photon reflected/scattered light imaging and multiphoton imaging can be achieved using the same lens. Such a capability is valuable for clinical applications. For example, one-photon reflected light or confocal imaging might be preferred for the low-magnification and large FOV survey, while multiphoton imaging might be optimum for high-resolution diagnosis. Further adjustment could be made for the FOVs and NAs in both optical zones in order to satisfy clinical application requirements.

In summary, a dual optical zone lens was designed, fabricated, and characterized. The feasibility of employing the dual-zone endoscope lens to achieve multiphoton/single-photon imaging with dual FOVs and resolutions was demonstrated. Such a dual-zone lens system could provide a practical solution for clinical *in vivo* imaging by locating diseased areas with its larger FOV and subsequently providing high-resolution clinical diagnosis without the need for any optical or mechanical adjustment of the endoscope.

Acknowledgments

This research was supported by the National Institutes of Health (NIH) grant 1 R01 EB006736-03. The authors would like to thank Mark Williams for the critical reading and insightful comments.

References

1. Denk W, Strickler JH, Webb WW. Science 1990;248:73. [PubMed: 2321027]
2. Zipfel WR, Williams RM, Webb WW. Nature Biotechnol 2003;21:1369. [PubMed: 14595365]
3. Jung JC, Schnitzer MJ. Opt Lett 2003;28:902. [PubMed: 12816240]
4. Wu Y, Leng Y, Xi J, Li XD. Opt Express 2009;17:7907. [PubMed: 19434122]
5. Fu L, Gan X, Gu M. Opt Express 2005;13:5528. [PubMed: 19498549]

6. Le Harzic R, Weinigel M, Riemann I, König K, Messerschmidt B. Opt Express 2008;16:20588. [PubMed: 19065197]
7. Wu Y, Xi J, Cobb MJ, Li XD. Opt Lett 2009;34:953. [PubMed: 19340182]
8. Birk DE, Trelstd RL. J Cell Biol 1986;103:231. [PubMed: 3722266]

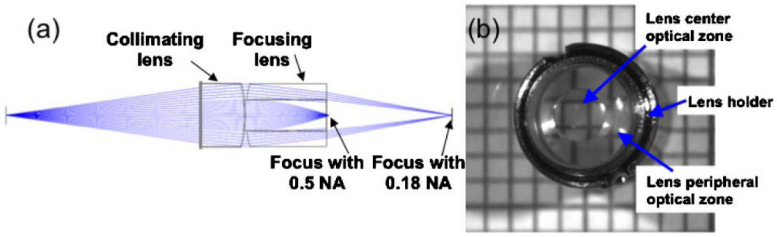

Fig. 1.

(Color online) (a) Ray tracing diagram of the optical properties of the bifocal lens assembly. (b) Top view of a bifocal lens assembly in a lens holder. The center and peripheral optical zones are indicated by the image circular truncation of an underlying grid pattern.

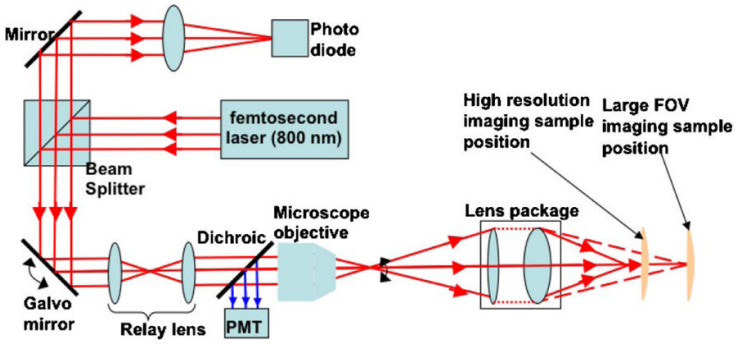

Fig. 2.
(Color online) Schematic diagram of the experiment setup for one-photon reflectance and multiphoton imaging.

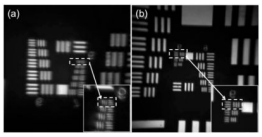

Fig. 3.
Reflection images of a USAF target measured with NAs of (a) 0.18 and (b) 0.5. The insets in (a) and (b) are magnified images of the bars highlighted by the square. For all images, a 1 Hz frame rate was used.

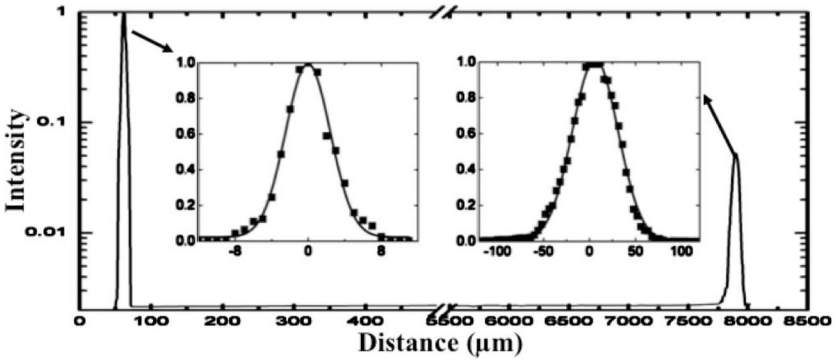

Fig. 4.

Fluorescence intensity axial profile (in logarithmic scale) of both foci through the center of a fluorescence bead along the axial direction. Normalized peak intensities with a solid line Gaussian fit are shown in inset figures.

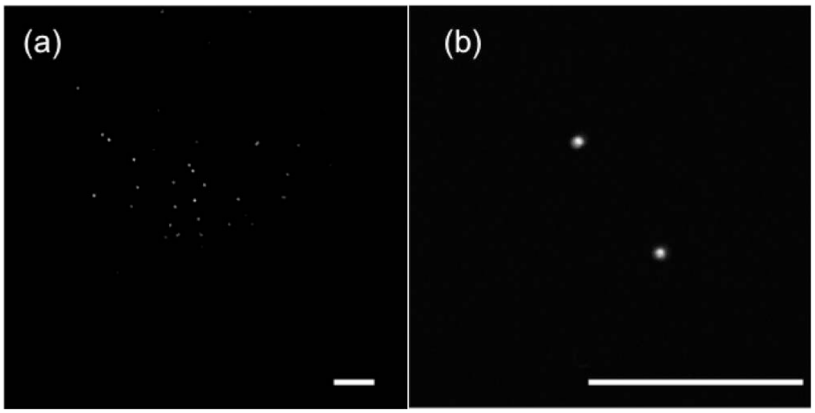

Fig. 5.
Multiphoton images of 6 μm beads fixed in agarose measured with 0.18 and 0.50 NA in (a) and (b), respectively. The horizontal scale bars are 100 μm.

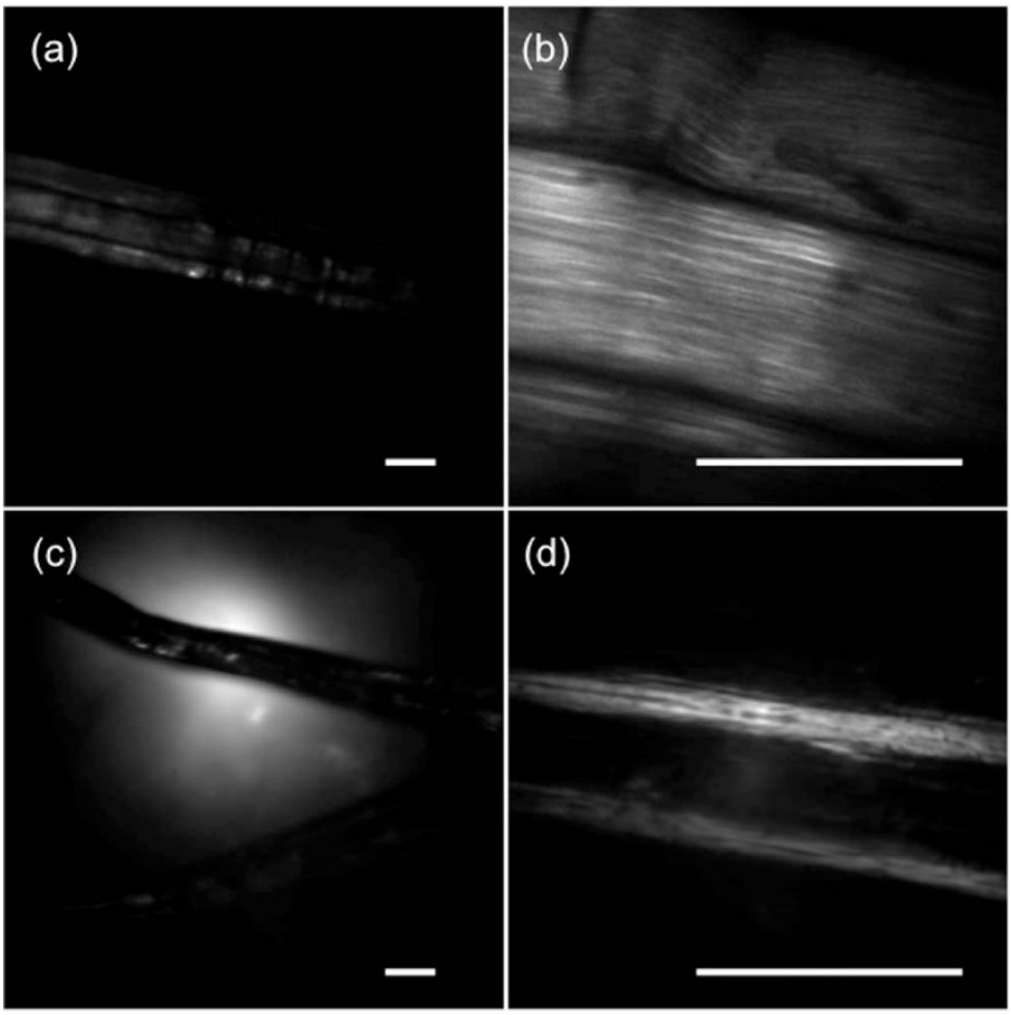

Fig. 6.
(a),(b) SHG and (c),(d) reflection images of a rat-tail tendon, acquired with (b),(d) 0.50 and (a),(c) 0.18 NA. The scale bars are 100 μm.